Monitoring of Wind Turbine Blades Based on Dual-Tree Complex Wavelet Transform

LIU Rongmei[1*], *ZHOU Keyin*[1], *YAO Entao*[2]

1. College of Aerospace Engineering, Nanjing University of Aeronautics and Astronautics, Nanjing 210016, P.R. China;
2. College of Automation Engineering, Nanjing University of Aeronautics and Astronautics, Nanjing 210016, P.R. China

(Received 7 December 2020; revised 30 January 2021; accepted 1 February 2021)

Abstract: Structural health monitoring (SHM) in-service is very important for wind turbine system. Because the central wavelength of a fiber Bragg grating (FBG) sensor changes linearly with strain or temperature, FBG-based sensors are easily applied to structural tests. Therefore, the monitoring of wind turbine blades by FBG sensors is proposed. The method is experimentally proved to be feasible. Five FBG sensors were set along the blade length in order to measure distributed strain. However, environmental or measurement noise may cover the structural signals. Dual-tree complex wavelet transform (DT-CWT) is suggested to wipe off the noise. The experimental studies indicate that the tested strain fluctuate distinctly as one of the blades is broken. The rotation period is about 1 s at the given working condition. However, the period is about 0.3 s if all the wind blades are in good conditions. Therefore, strain monitoring by FBG sensors could predict damage of a wind turbine blade system. Moreover, the studies indicate that monitoring of one blade is adequate to diagnose the status of a wind generator.

Key words: wind turbine blade; structural health monitoring (SHM); fiber Bragg grating (FBG); dual-tree complex wavelet transform (DT-CWT)

CLC number: TP29 **Document code:** A **Article ID:** 1005-1120(2021)01-0140-13

0 Introduction

Wind power is becoming one of the fastest growing energy technologies in the world[1]. However, generation cost may be extra increased due to annual operating costs, such as maintenance on the generation systems[2]. Therefore, a reliable structural health monitoring (SHM) system is pressing needed for the successful implementation of wind turbine systems[3].Du et al. reviewed damage detection techniques for blades[4].

Wind turbine blades are among the most easily damaged parts of a turbine system because of the working environment. Blade failure would be catastrophic. Therefore, it is critical to detect blade damages at their early stage. Periodic inspections are proposed to reduce the probability of complete blade failures[5].

Lee et al. monitored the blade deflection based on strain gauge sensors[6]. Dilek et al. studied monitoring of blades by an automated laser scanning system[7]. Procházka et al. used magneto-resistive sensors to study strain and damage of steam turbine blade[8]. It was pointed out that monitoring of dynamic characteristics, such as amplitudes and frequencies of vibrations, could represent a fundamental damage assessment for turbine blades[9]. The proposed method was based on analysis of structural resonance[10]. Finite element analyses were suggested to study the behavior of wind turbine blade[11-12]. The analyses and supported tests on designed wind turbine blades implicated that the lamination of the outer skin was the initial destruction. It followed by lamination buckling which led to breakdown of the generation.

Non-destructive testing (NDT) techniques

*Corresponding author, E-mail address: romme@nuaa.edu.cn.

How to cite this article: LIU Rongmei, ZHOU Keyin, YAO Entao. Monitoring of wind turbine blades based on dual-tree complex wavelet transform[J]. Transactions of Nanjing University of Aeronautics and Astronautics, 2021, 38(1): 140-152.
http://dx.doi.org/10.16356/j.1005-1120.2021.01.014

were proposed to detect damage in composite blades. These techniques, including visual inspection or acoustic emission[13], were labor intensive, or difficult to be used because of testing noise during operation. Besides, extended time was required to access the blade[14]. However, the above mentioned studies indicated that surface dynamic characters monitoring could help detect blade fault.

Optical fiber possesses the advantages of immunity to electromagnetic interference, corrosion resistance, and so on[15]. Therefore, optical fiber based sensors have increasingly applied to SHM in their total life cycles[16-18]. Among the optical fiber sensors, fiber Bragg grating (FBG) sensors are proposed increasingly for strain monitoring in structures because of their real time response, accurate performance[19-22].

Mieloszyk et al. used a SHM system based on FBG sensors on a wind turbine model[23]. According to the results by Ref.[11], monitoring of the outer skin of a blade is essential. Therefore, FBG sensors were assigned on the blade surfaces of a wind turbine. The dynamic behavior of wind turbine system was monitored. Measured noise caused by background and wind turbines noise would indistinct the data[24-25]. Therefore, an algorithm based on dual-tree complex wavelet transform (DT-CWT) is proposed to remove the system noise. The methodology is verified by experiments.

1 Methodology

Not just the wind turbine performance but its safety would be affected by wind evidently[26]. Accordingly, wind loaded turbine systems are studied. The structural responses are monitored by FBG sensors.

Before the blade is fixed on a hub, five FBG sensors are glued on its surface. All the sensors are joined together and connected to broadband source (BBS) and demodulator. The sense principle is sketched in Fig.1.

To simplify the analysis, the working blade on the hub is considered as a cantilever. The blowing wind on the turbine can be simplified as uniform load at any moment. The computing model for a rotating blade at any instance is sketched in Fig.2.

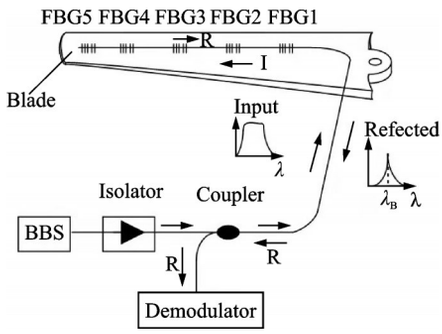

Fig.1 Sketch of the sensing principle

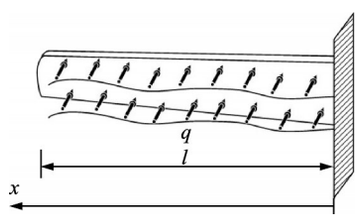

Fig.2 Schematic diagram of a rotating blade at any instance

Therefore, the strain along the blade, i.e. $\varepsilon(x)$ distributes as follows

$$\varepsilon(x)=\frac{q(l-x)^2}{2EW(x)} \tag{1}$$

where the parameters E and $W(x)$ are Young's modulus and section modulus in bending, respectively.

When a FBG sensor is connected to a broadband source, a light travels through the FBG sensors. The light will interact with FBG sensors. Afterwards, a narrow-band spectral output at the sensor, which is known as the Bragg wavelength, will be reflected. The reflected Bragg wavelength is determined by the well-known formula[27]

$$\lambda_B=2n_{eff}\Lambda \tag{2}$$

where the parameters λ_B, n_{eff} and Λ are the Bragg grating wavelength, the effective refractive index and the average grating period of the FBG, respectively.

As the physical parameter on the blade changes, the parameters n_{eff} and Λ will change. At the assumption of no temperature change, the Bragg wavelength will change with axial strain. The axial strain at position x is time variable and denoted as $\varepsilon(x, t)$. The wavelength shift $\Delta\lambda_B$ can be expressed

in the form[28]

$$\frac{\Delta\lambda_B}{\lambda_B}=S_\varepsilon\varepsilon(x,t) \tag{3}$$

where S_ε is the relative strain sensitivity of a FBG. For the common used FBG, the core is made of silicon oxide. Hence, the sensitivity S_ε is 0.784.

As the wind turbine works, the strain on the blade will change with time. For a given detected point on the blade, the time variable strain $\varepsilon(t)$ is captured by FBG sensor. Consequently, the monitored strain value can be obtained by

$$\varepsilon(t)=\frac{1}{\lambda_B(\varepsilon_0,t_0)\cdot S_\varepsilon}\left[\lambda_B(\varepsilon,t)-\lambda_B(\varepsilon_0,t_0)\right] \tag{4}$$

where the parameters $\lambda_B(\varepsilon_0, t_0)$ and $\lambda_B(\varepsilon, t)$, are the original and changed FBG wavelengths, respectively.

However, noise would disguise the strain variation during blade vibration. Wavelet transform was applied to condition monitoring and denoising diagnostics[29].

Many different techniques, such as discrete wavelet transform (DWT), second-generation wavelet transform (SGWT), empirical mode decomposition (EMD), etc., have been proposed. Nevertheless, DT-CWT consistently outperforms others[30]. This method enjoys many attractive properties including nearly shift invariance and reduced aliasing. The properties may be favorable to both the surveillance and diagnosis of rotating machinery.

Therefore, an algorithm based on DT-CWT was proposed to reduce the noise and to extract the dynamic signals. By using dual-tree of wavelet filters, the real and imaginary parts of the signal could be obtained. Therefore, limited redundancy was introduced and computational efficiency was preserved[31].

The captured signal $\varepsilon(t)$ is discretized by a set of wavelets[32]

$$\varepsilon(t)=\sum_{n=-\infty}^{\infty}c(n)\phi(t-n)+\sum_{j=0}^{\infty}\sum_{n=-\infty}^{\infty}d(j,n)2^{j/2}\psi(2^jt-n) \tag{5}$$

where $\phi(t)$ and $\psi(t)$ represent the scaling functions and the band-pass wavelets, respectively. $c(n)$ and $d(j, n)$ are the associated scaling coefficients and the wavelet coefficients, and they can be obtained by the following equations

$$c(n)=\int_{-\infty}^{\infty}\varepsilon(t)\phi(t-n)\mathrm{d}t \tag{6}$$

$$d(j,n)=2^{j/2}\int_{-\infty}^{\infty}\varepsilon(t)\psi(2^jt-n)\mathrm{d}t \tag{7}$$

The wavelets and scaling functions, i.e. $\psi(t)$ and $\phi(t)$, are complex-valued. The real and imaginary parts of the wavelets $\psi(t)$ form a Hilbert transform pair. Therefore, the complex-valued wavelet is an analytic signal.

The above mentioned transform is approximate shift invariant. This feature is very important in pattern recognition and signal analysis[33]. In the transformation, two separate real discrete bases $\psi_r(t)$ and $\psi_i(t)$, i.e. the real and imaginary parts of the wavelets $\psi(t)$, are used. They are two individually orthonormal wavelet transforms.

Consequently, the complex wavelet coefficient $d(j, n)$, can be obtained by projecting the signal $\varepsilon(t)$ onto $2^{j/2}\psi(2^jt-n)$[34].

The coefficients, i.e. real and imaginary parts of $d(j, n)$, are filtered individually. The approach is based on two filter bank trees and thus on two bases. Afterwards, a new complex wavelet coefficient $d_{cnew}(j, n)$ could be obtained by using the original phase and new wavelet magnitude

$$d_{cnew}(j,n)=m_d e^{i\alpha} \tag{8}$$

where m_d and α are the filtered magnitude and the original phase, respectively.

2 Experimental Setup

An experimental program is designed to evaluate the efficiency of the proposed methodology. The wind turbine (type of NE-100S), as shown in Fig.3(a), is developed by Jiangsu Naier Wind Power Technology Development Co., Ltd. The length of each blade is 550 mm. Three blades are mounted on a hub. The diameter of the hub is 200 mm. FBG sensors are glued on blade surfaces. A commercial FBG demodulator from Micron Optics (model # SM130), as shown in Fig.3(b), is used in experiments to capture strain data.

Behaviors of two blade systems are studied experimentally. For the first kind, all the blades are in good conditions. Five FBG sensors are glued on one

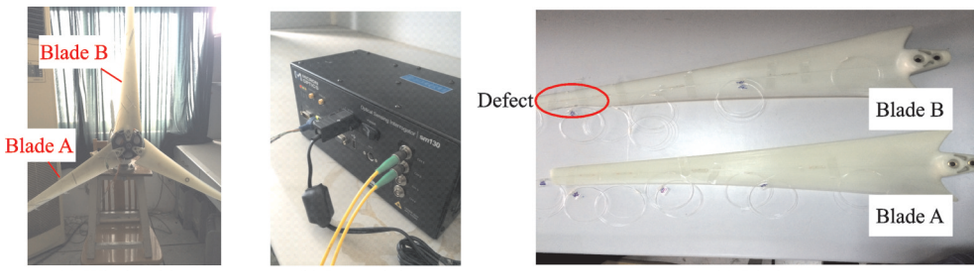

(a) Wind turbine (b) Demodulator (c) Blades

Fig.3 Schematic of experimental setup for wind blade monitoring

of the blades. The monitored blade is denoted as Blade A. For the second kind, one of the good blades, except Blade A, is replaced by Blade B. For Blade B, the free end is broken. Blade A and Blade B are shown in Fig.3. The details of the two blades are shown in Table 1.

Table 1 Original details of FBG sensors

Sensor	Distance from fixed end/mm	Original central wavelength of Blade A/ nm	Original central wavelength of Blade B/ nm
FBG1	100	1 512.13	1 512.11
FBG2	200	1 525.11	1 525.11
FBG3	350	1 529.87	1 529.83
FBG4	450	1 549.81	1 549.79
FBG5	500	1 555.13	1 555.23

The original spectrums of the FBG sensors on Blade A is shown in Fig.4.

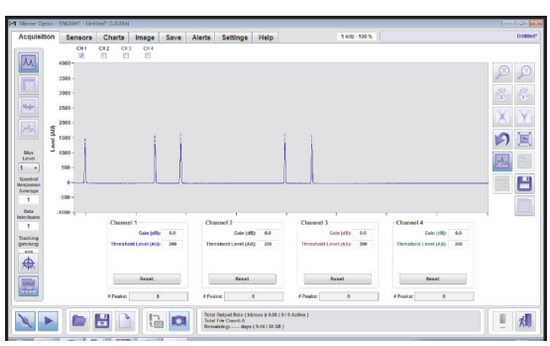

Fig.4 Original spectrums of the FBG sensors on Blade A

After the blades are fixed on the hub, the whole system is wind loaded by an electric fan. The blowing velocity is 2.4 m/s.

For a real scale wind turbine, it may not rotate if the wind velocity is too small. In order to well understand a real scale wind turbine, two working conditions are considered. Firstly, no rotation of the blades is allowed by fixing the hub as it is subjected to wind. Secondly, the blades are set free and they can spin under wind load.

3 Testing Results

As the blades are wind loaded, they will deform. The central wavelengths of the glued FBG sensors will change and be recorded by the demodulator. The captured strain data can be obtained according to Eq.(4).

3.1 Blowing with fixed hub

As the wind turbine does not spin around the hub, the monitored results by FBG sensors are presented in Figs.5 and 6.

As shown in Fig.5, if all the blades are in good conditions, the data oscillate evenly with wind. For the values of FBG5, both the peak value and the valley one are 1 micro-strain smaller than those of other FBGs. The strain curve offset down integrally. The testing error may be caused by the instrument. The testing error for the FBG demodulator is about 1 micro-strain.

If one of the blades is broken, the testing results on different blades are displayed in Fig.6. The data goes up and down obviously even if the hub is fixed.

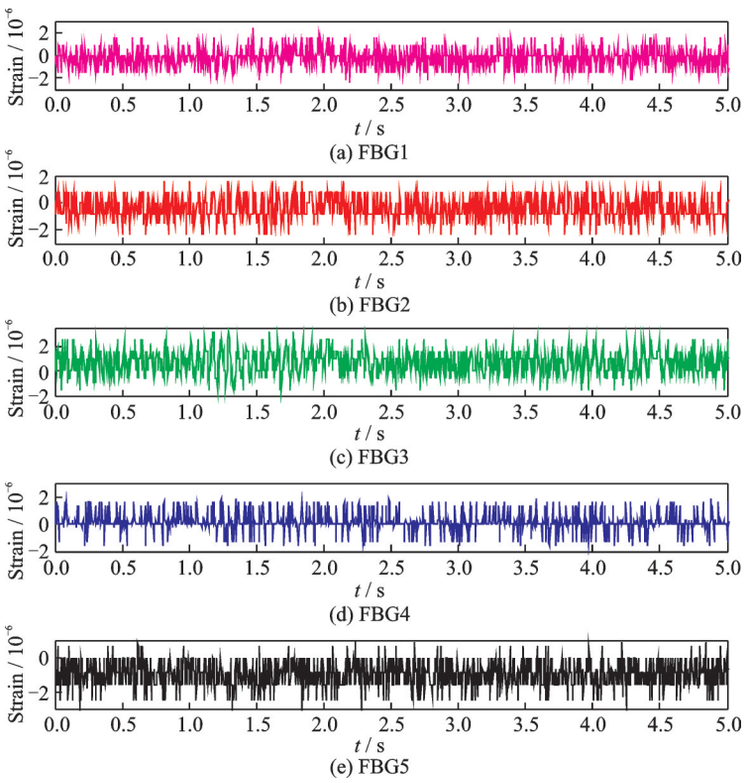

Fig.5 Results on Blade A as all the blades are in good conditions as the hub is fixed

3.2 Blowing freely

At the same blowing velocity, the monitored results when the turbine rotates about the hub are shown in Figs.7 and 8.

Shown in Fig. 7 are strain data monitored by the FBG sensors on Blade A, as all the blades are in good conditions. Obviously, the stain of FBG5 is smaller than others. The reason lies in the position of FBG5. FBG5 is glued near to the free end of the cantilever. Consequently, the structural strain is smaller.

The strain data on Blade A and Blade B, as Blade B is broken, are displayed in Fig.8. The data on Blade A shares the same change with Blade

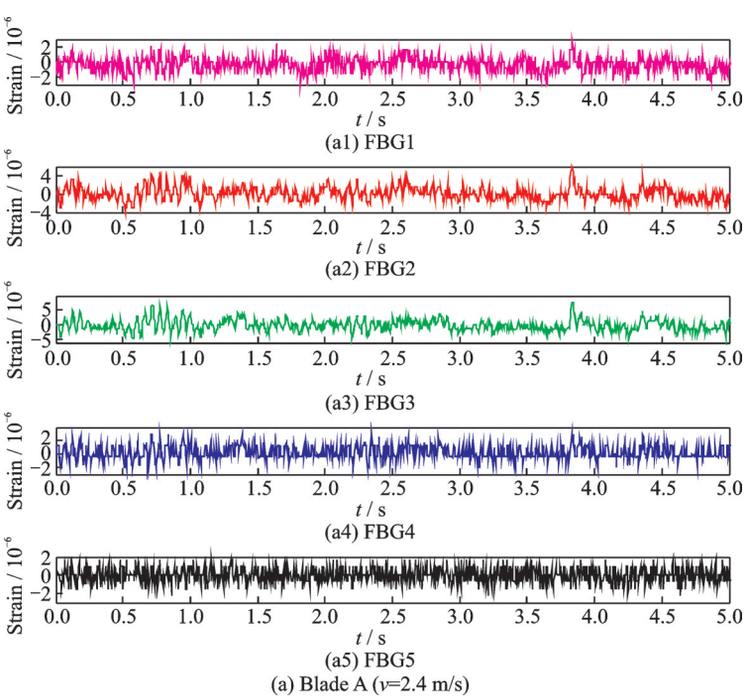

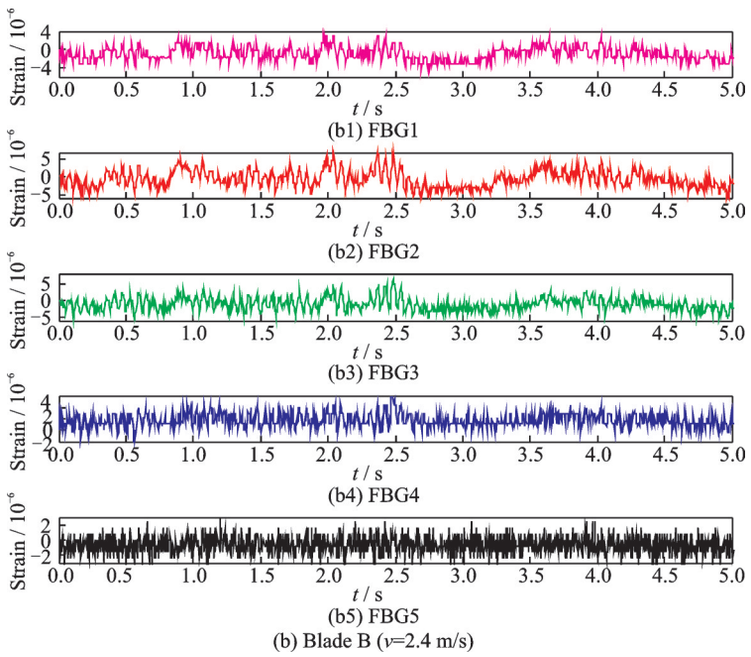

Fig.6 Results as Blade B is broken with fixed hub

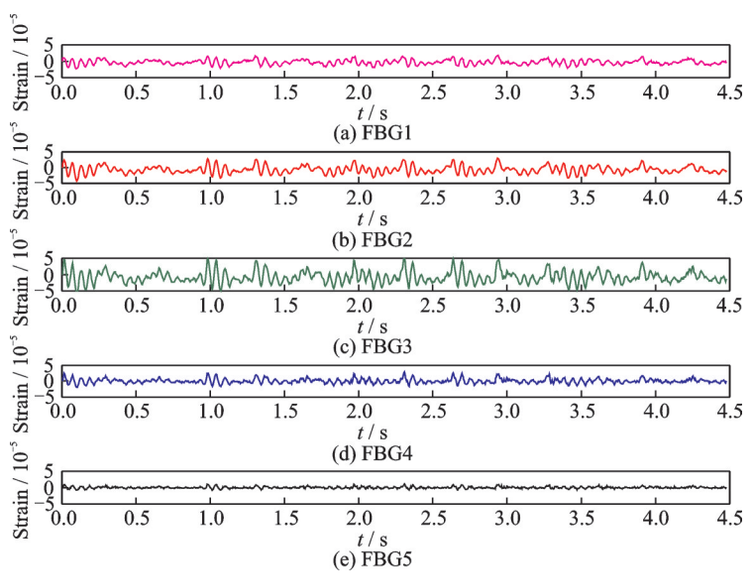

Fig.7 Monitored strain data as all rotating blades are in good conditions

B at the same position. Nevertheless, the value is different at the same time. The initial variation trend is different during the testing for each blade. It is caused by different deformation on different blades. In the first 0.5 s, the testing surface of Blade A is undergoing increasing compressed. However, the surface of Blade B is gradually elongated.

The strain data on Blade A change with time apparently when all the blades are in good conditions. As one of the blades is broken, the data variation is more obvious as shown in Fig.8(a) compared with Fig.7.

In order to study the strain character further more, the timely strain data is discretized, filtered and recomposed.

3.3 Data processing

The captured strain data is processed in order to extract the feature during turbine rotation.

Firstly, the strain data is discretized into four layers of wavelets after Hilbert transformation. The real and imaginary parts of the wavelet coefficients,

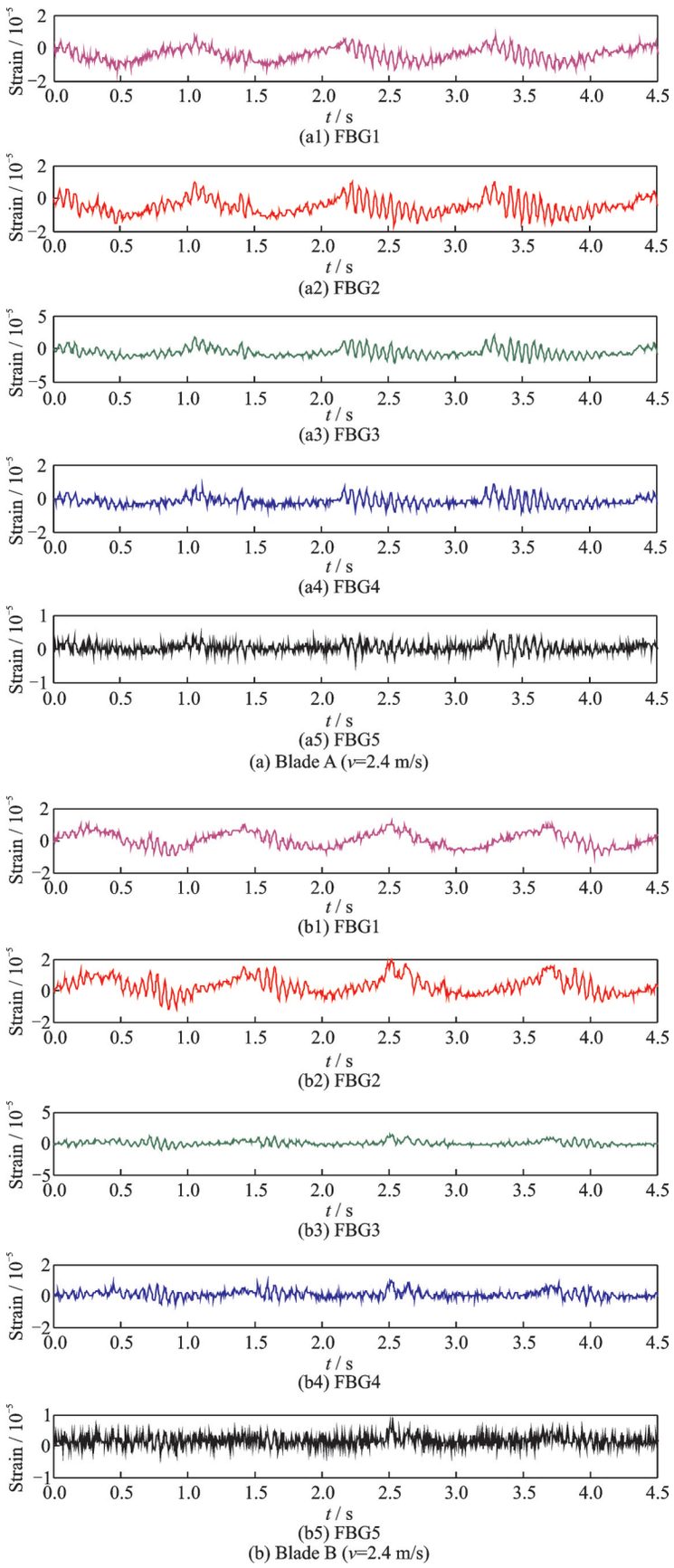

Fig.8 Strain data on rotating Blades A & B as Blade B is broken

as all the blades are in good conditions, are indicated in Figs.9(a) and (b), respectively. In Figs.9(a) and (b), the horizontal and vertical axes represent numbers and amplitudes for four layers, respectively.

Secondly, the real and imaginary parts of the coefficients are filtered, respectively. Afterwards, the wavelet coefficients are obtained according to Eq.(8) and the result is sketched in Fig.10. The vertical axes, d_1—d_4, represent amplitudes in four different subbands.

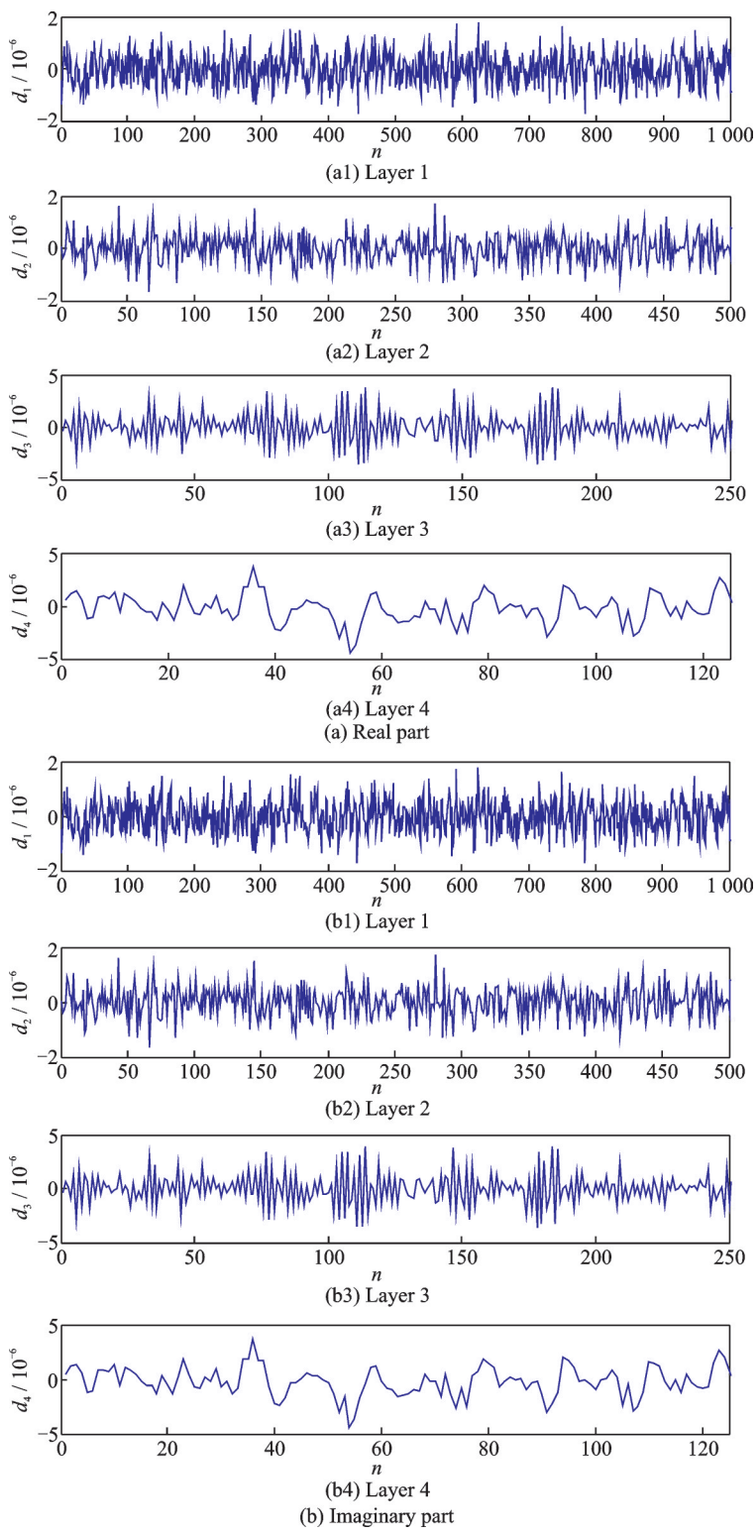

Fig.9 Wavelet coefficients after Hilbert transformation

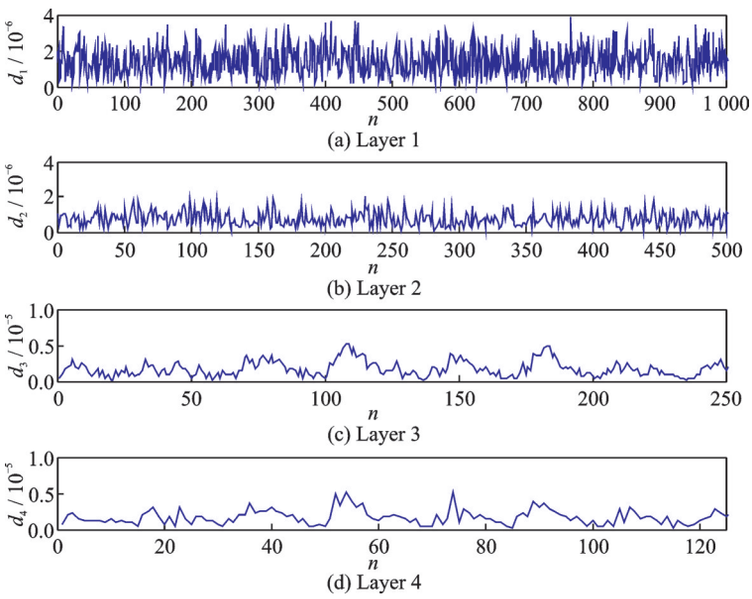

Fig.10 Mode of the filtered wavelet coefficient

Finally, the signal is reconstructed according to Eqs.(5—8).

The reconfigured strain at each monitoring point as all the blades are good is illustrated in Fig.11.

It is obviously in Fig.11 that strain on each site varies similarly. It is all but periodical changes during the wind turbine blade rotation. The period for individual point is about 0.3 s. The strain values are almost the same except for the points detected by FBG4 and FBG5. The reason lies in that the bending moment is very small near the free end of the blade, whose value is zero at the free end. The equal strain illustrates that the blade is designed with an uniform strength.

The strain data for another blade system is processed and illustrated in Fig.12.

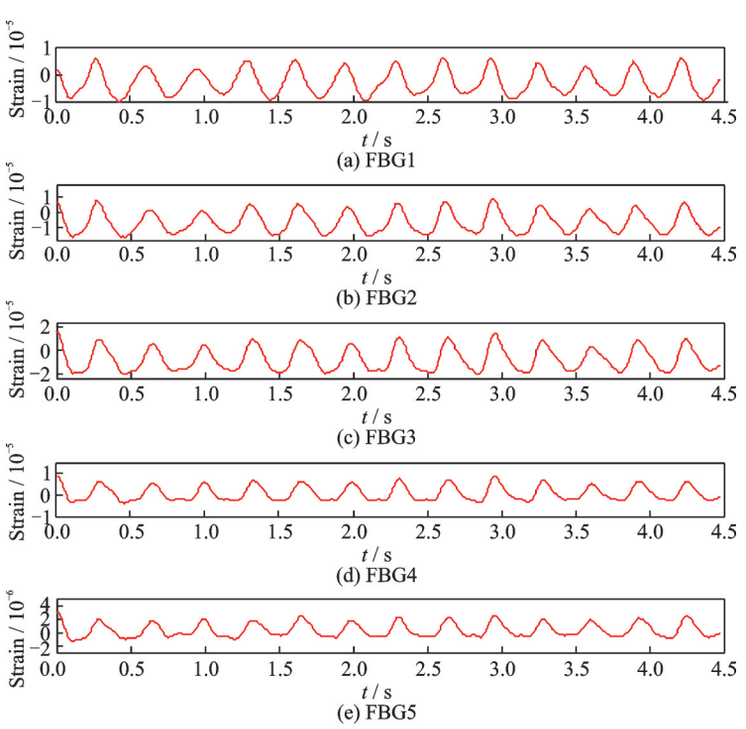

Fig.11 Processed strain data on Blade A as all blades are good

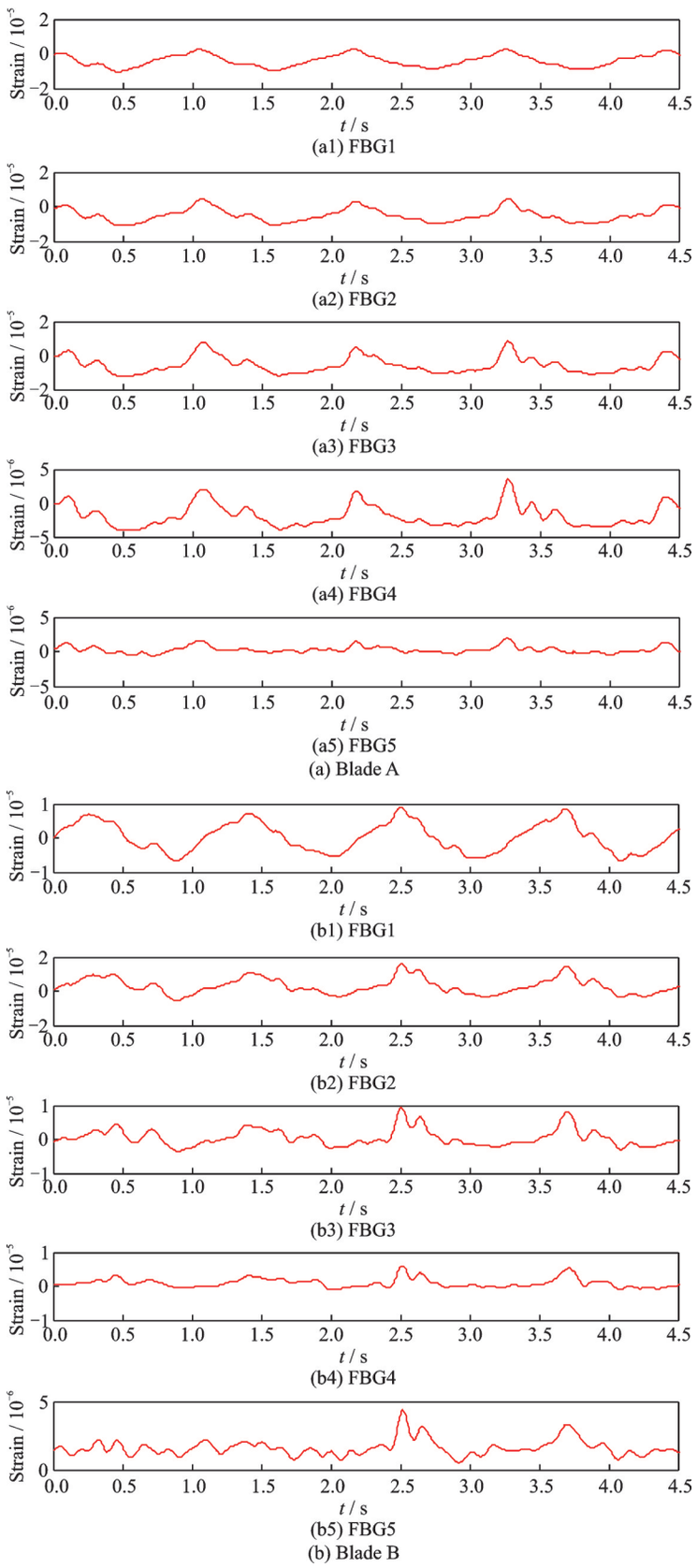

Fig.12 Processed strain on Blades A & B as Blade B is broken

Apparently, the strain data fluctuate as one of the blades is broken. The strain shares similar variety for each point on the same blade.

For Blade A and Blade B, the turn periods are

all about 1 s.

Obviously, the good blade shares similar dynamic character with the broken one. Therefore, it could be concluded that detection of one blade is sufficient for health monitoring of the whole wind turbine.

4 Conclusions

A non-destructive evaluation technique of wind blade SHM was investigated. The technique includes application of FBG sensors.

When the wind turbine rotates, the strain on blade changes periodically. The gravity of the blades may affect the strain value. However, it would not cover the variation trend. If one of the blades is broken, the strain fluctuates apparently. Furthermore, periods of strain change will be different. The reason lies in the structural inherent frequency change caused by broken blade. Therefore, variation of strain period or frequency could be a reference for SHM.

According to the tests, no matter whether the turbine revolves or not, the strain difference could be monitored by the proposed method.

The experimental testing results indicate that sensing of one blade is adequate for monitoring the whole wind turbine in service. On the blade being monitored, one FBG sensor is enough for the job. However, the sensor should be placed far away from the free end.

References

[1] XIAO F, TIAN C, WAIT I, et al. Condition monitoring and vibration analysis of wind turbine[J]. Advances in Mechanical Engineering, 2020, 12(3): 1-9.

[2] LICARI J, UGALDE-LOO C E, EKANAYAKE J B, et al. Comparison of the performance and stability of two torsional vibration dampers for variable-speed wind turbines[J]. Wind Energy, 2015, 18(9): 1545-1559.

[3] LIAN J J, CAI O, DONG X F, et al. Health monitoring and safety evaluation of the offshore wind turbine structure: A review and discussion of future development[J]. Sustainability, 2019, 11(2): 494.

[4] DU Y, ZHOU S X, JING X J, et al. Damage detection techniques for wind turbine blades: A review[J]. Mechanical Systems and Signal Processing, 2019, 141: 106445.

[5] NIELSEN J S, TCHERNIAK D, ULRIKSEN M D. A case study on risk-based maintenance of wind turbine blades with structural health monitoring[J]. Structure and Infrastructure Engineering, 2020. DOI: 10.1080/15732479.2020.1743326.

[6] LEE K, AIHARA A, PUNTSAGDASH G, et al. Feasibility study on a strain based deflection monitoring system for wind turbine blades[J]. Mechanical Systems and Signal Processing, 2017, 82: 117-129.

[7] DILEK A U, OGUZ A D, SATIS F, et al. Condition monitoring of wind turbine blades and tower via an automated laser scanning system[J]. Engineering Structures, 2019, 189: 25-34.

[8] PROCHÁZKA P, VANĚK F. Contactless diagnostics of turbine blade vibration and damage[J]. Journal of Physics: Conference Series, 2011, 305: 012116.

[9] SARRAFI A, ZHU M. Wind turbine blade damage detection via 3-dimensional phase-based motion estimation[C]//Proceedings of the 11th International Workshop on Structural Health Monitoring. Stanford, United states: [s.n.], 2017: 2545-2552.

[10] ZHANG L A, TAO L M, WEI X T, et al. Multi-axis fatigue loading system of wind turbine blade and vibration coupling characteristics[J]. Journal of Vibroengineering, 2017, 19(1): 1-13.

[11] BENDER J J, HALLETT S R, LINDGAARD E. Investigation of the effect of wrinkle features on wind turbine blade sub-structure strength[J]. Composite Structures, 2019, 218: 39-49.

[12] YEH M K, WANG C H. Stress analysis of composite wind turbine blade by finite element method[C]//Proceedings of the 5th Asia Conference on Mechanical and Materials Engineering. Tokyo, Japan: Iop Publishing Ltd, 2017, 241: 012015.

[13] YANG K, RONGONG J A, WORDEN K. Damage detection in a laboratory wind turbine blade using techniques of ultrasonic NDT and SHM[J]. Strain, 2018, 54(6): e12290.

[14] GHOSHAL A, SUNDARESAN M J, SCHULZ M J, et al. Structural health monitoring techniques for wind turbine blades[J]. Journal of Wind Engineering and Industrial Aerodynamics, 2000, 85: 309-324.

[15] HU X L, SHI Z X, WANG Y, et al. Packaging and characteristics of a tapered fiber sensor for refractive-index measurements[J]. Journal of Russian Laser Re-

search, 2018, 39(2): 200-206.

[16] JIANG Y, ZHANG M. Influence of light source on the strain sensitivity of a polarisation maintaining fibre loop mirror based on voltage demodulation[J]. IET Optoelectronics, 2019, 13(3): 109-112.

[17] ZHANG X L, WANG P, LIANG D K, et al. A soft self-repairing for FBG sensor network in SHM system based on PSO-SVR model reconstruction[J]. Optics Communications, 2015, 343: 38-46.

[18] LIU R M, MENG D, LI Z. Study on defects detection of a structure undergoing dynamic load[J]. Journal of Vibroengineering, 2015, 17(4): 1828-1836.

[19] HSU T Y, SHIAO S Y, LIAO W I. Damage detection of rotating wind turbine blades using local flexibility method and long-gauge fiber Bragg grating sensors[J]. Measurement Science & Technology, 2018, 29(1): 015108.

[20] BAO T, BABANAJAD S K, TAYLOR T, et al. Generalized method and monitoring technique for shear strain based bridge weigh in motion[J]. Journal of Bridge Engineering, 2015, 21(1): 1-13.

[21] LENG J S, ASUNDI A. Structural health monitoring of smart composite materials by using EFPI and FBG sensors[J]. Sensors and Actuators A, 2003, 103(3): 330-340.

[22] LIU R, LIANG D. Natural frequency detection of smart composite structure by small diameter fiber Bragg grating[J]. Journal of Vibration and Control, 2015, 21(14): 2896-2902.

[23] MIELOSZYK M, OSTACHOWICZ W. An application of structural health monitoring system based on FBG sensors to offshore wind turbine support structure model[J]. Marine Structures, 2017, 51: 65-86.

[24] GALLO P, FREDIANELLI L, PALAZZUOLI D, et al. A procedure for the assessment of wind turbine noise[J]. Applied Acoustics, 2016, 114: 213-217.

[25] LIU Z, ZHANG L. Naturally damaged wind turbine blade bearing fault detection using novel iterative nonlinear filter and morphological analysis[J]. IEEE Transactions on Industrial electronics, 2020, 67(10): 8713-8722.

[26] JANG Y J, CHOI C W, LEE J H, et al. Development of fatigue life prediction method and effect of 10-minute mean wind speed distribution on fatigue life of small wind turbine composite blade[J]. Renewable Energy, 2015, 79: 187-198.

[27] RAZALI N F, ABUBAKAR M H, TAMCHEK N, et al. Fiber Bragg grating for pressure monitoring of full composite lightweight epoxy sleeve strengthening system for submarine pipeline[J]. Journal of Natural Gas Science and Engineering, 2015, 26: 135-141.

[28] LU S, JIANG M, SUI Q, et al. Low velocity impact localization system of CFRP using fiber Bragg grating sensors[J]. Optical Fiber Technology, 2015, 21: 13-19.

[29] DALPIAZ G, RIVOLA A. Condition monitoring and diagnostics in automatic machines: Comparison of vibration analysis techniques[J]. Mechanical Systems and Signal Processing, 1997, 11(1): 53-73.

[30] WANG Y, HE Z, ZI Y. Enhancement of signal denoising and multiple fault signatures detecting in rotating machinery using dual-tree complex wavelet transform[J]. Mechanical Systems and Signal Processing, 2010, 24(1): 119-137.

[31] CHEN L, WANG J J, SUN B. Facial expression recognition based on the Q-shift DT-CWT and rotation invariant LBP[J]. Journal of Donghua University (English Edition), 2012, 29(1): 71-75.

[32] CHAKRABORTY S, BHATTACHARYA I, CHATTERJEE A. A palm print based biometric authentication system using dual tree complex wavelet transform[J]. Measurement, 2013, 46 (10): 4179-4188.

[33] CHEN G. Automatic EEG seizure detection using dual-tree complex wavelet-Fourier features[J]. Expert Systems with Applications, 2014, 41(5): 2391-2394.

[34] QU J, ZHANG Z, GONG T. A novel intelligent method for mechanical fault diagnosis based on dual-tree complex wavelet packet transform and multiple classifier fusion[J]. Neurocomputing, 2015, 171(1): 837-853.

Acknowledgements This work was supported by the National Natural Science Foundation of China (No.11402112) and the National Key Technology Support Program (No. 2012BAA01B02).

Author Dr. **LIU Rongmei** received the B.S. and M.S. degrees in Materials Science and Engineering from Nanjing University of Aeronautics and Astronautics (NUAA) in 1997 and 2000, respectively. In 2011, she obtained her Ph.D. degree in Testing. She chose smart materials as her area of specialization. From 2002 to present, she has been with the College of Aerospace Engineering, NUAA. Her research has focused on optical fiber based sensors.

Author contributions Dr. **LIU Rongmei** designed the study, provided the core idea and wrote the manuscript.

Prof. **ZHOU Keyin** contributed to the discussion and background of the study. Prof. **YAO Entao** assisted in writing the manuscript. All authors commented on the manuscript draft and approved the submission.

Competing interests The authors declare no competing interests.

(Production Editor: XU Chengting)

基于双树复小波变换的风力叶片监测研究

刘荣梅[1], 周克印[1], 姚恩涛[2]

(1.南京航空航天大学航空学院,南京 210016,中国; 2.南京航空航天大学自动化学院,南京 210016,中国)

摘要:对风力发电系统而言,结构服役期间的健康监测非常重要。由于布拉格光纤光栅(Fiber Bragg grating, FBG)传感器的中心波长随应变或温度呈线性变化,因此FBG传感器广泛应用于结构测试。本文提出了基于FBG传感器的风力叶片监测方法,并通过实验验证该方法。沿着叶片长度方向粘贴5个FBG传感器进行应变测量。由于环境及测试噪声会掩盖结构真实信号,文中采用双树复小波变换(Dual-tree complex wavelet transform, DT-CWT)方法,进行数据处理,滤去噪声信号。实验验证结果表明,当其中一根叶片出现损坏时,测量应变出现明显波动,给定工作条件下,旋转周期为1 s,而结构完好时的周期为0.3 s。因此,利用布拉格光纤光栅传感系统进行应变测量,可以预测风力叶片系统的损坏。进一步研究表明,可以通过监测其中一根叶片,从而对整个风力发电系统进行故障预测。

关键词:风力发电机叶片;结构健康监测;布拉格光纤光栅;双树复小波变换